



# Effect of chemical etching by sulfuric acid or H<sub>2</sub>O<sub>2</sub> NH<sub>3</sub> mixed solution on the photocatalytic activity of rutile TiO<sub>2</sub> nanorods

著者	Bae Eunyoung, Murakami Naoya, Nakamura Misa, Ohno Teruhisa
journal or publication title	Applied Catalysis A: General
volume	380
number	1-2
page range	48-54
year	2010-05-31
URL	<a href="http://hdl.handle.net/10228/00006581">http://hdl.handle.net/10228/00006581</a>

doi: [info:doi/10.1016/j.apcata.2010.03.029](https://doi.org/10.1016/j.apcata.2010.03.029)

**Effect of Chemical Etching by Sulfuric Acid or H<sub>2</sub>O<sub>2</sub>-  
NH<sub>3</sub> Mixed Solution on the Photocatalytic Activity of Rutile TiO<sub>2</sub>  
Nanorods**

Eunyoung Bae, Naoya Murakami, and Teruhisa Ohno\*

*Department of Materials Science, Faculty of Engineering, Kyushu Institute of  
Technology, 1-1 Sensuicho, Tobata-ku, Kitakyushu 804-8550, Japan*

Submitted to

*Applied Catalysis A: General*

February 2010

---

\*Corresponding author e-mail: [tohno@che.kyutech.ac.jp](mailto:tohno@che.kyutech.ac.jp)

Phone: +81-93-884-3318; Fax: +81-93-884-3318

## **Abstract**

Rutile TiO<sub>2</sub> nanorods synthesized by hydrothermal treatment were etched by addition of H<sub>2</sub>O<sub>2</sub>-NH<sub>3</sub> or H<sub>2</sub>SO<sub>4</sub> solution. The etched rutile TiO<sub>2</sub> nanorods were characterized by TEM, SEM, XRD, and specific surface area measurements. New crystal faces were generated on rutile TiO<sub>2</sub> nanorods by means of chemical etching. In the case of treatment with H<sub>2</sub>O<sub>2</sub>-NH<sub>3</sub> solution, the shape of the rutile TiO<sub>2</sub> nanorod changed to a sepal-like structure with reaction time. The dissolution of rutile TiO<sub>2</sub> nanorod mainly proceeded along [001] direction. When treated with sulfuric acid, the end [(111) face] of the rutile TiO<sub>2</sub> nanorod was gradually etched. The rutile TiO<sub>2</sub> nanorod finally exposed (001) and (021) faces during prolonged treatment time. In both cases, rutile TiO<sub>2</sub> nanorods were differently etched. The etched rutile TiO<sub>2</sub> nanorod showed higher photocatalytic activity for degradation of toluene in gas phase than the original particles.

## 1. Introduction

TiO<sub>2</sub> photocatalysts have been the focus of much attention due to their high photocatalytic activity as well as their chemical stability. The photocatalytic activity of TiO<sub>2</sub> is the result of an interaction among a series of parameters such as phase composition, electronic structure, particle size, exposed surface area, degree of aggregation, mobility of charge carriers and adsorption of molecules from gas or aqueous phase [1]. It is therefore important to develop a method to understand and control those properties due to the plurality of variables driving the nature of photocatalytic activity. In this work, the effect of chemical etching of nanoparticles was investigated. Among the various polymorphs of TiO<sub>2</sub>, rutile TiO<sub>2</sub> has some advantages over anatase, such as higher chemical stability and higher refractive index. It is of fundamental significance to explore mild synthetic techniques by which particle shapes, nano- and micro-meter-scale morphologies, and crystallinity are well defined and controlled [2-4]. Moreover, surface chemistry of single crystalline rutile particles has been the subject of intensive studies because their chemical activity depends greatly on surface structures [5].

Etching of nanoparticles has been discussed in previous reports. Whetten reported selective etching of particles on the basis of differences in their chemical

reactivity due to, for example, variations in defect density and surface faceting [6]. As concerns the modification of the surface structure of  $\text{TiO}_2$ , attempts to enlarge the surface areas of various materials have been made using various surface etching processes such as a photoelectrochemical etching process in aqueous sulfuric acid [7, 8]. A conventional chemical process for etching  $\text{TiO}_2$  is immersion in concentrated sulfuric acid at a high temperature. In addition, Taguchi et al. reported that HF and hot sulfuric acid treatment resulted in the formation of new crystal faces on both rutile and anatase  $\text{TiO}_2$  particles [9]. Moreover, Ohtani et al. reported that aqueous hydrogen peroxide ( $\text{H}_2\text{O}_2$ ) – ammonia ( $\text{NH}_3$ ) treatment gave a pure anatase crystalline phase from Degussa P25 containing both anatase and rutile crystallites [10]. Indeed, this technique can be used to separate anatase particles by selective dissolution of rutile. Here, we report that each of these chemical treatments leads to the formation of new crystal faces on rutile  $\text{TiO}_2$  particles.

Chemical etching of rutile  $\text{TiO}_2$  nanoparticles was carried out in this work. Chemical etching can be used to increase the number of new exposed crystal faces, especially in the case of  $\text{H}_2\text{SO}_4$ , similar to the process reported for synthesis using PVP. Exposed crystal face-selective etching of  $\text{TiO}_2$  in  $\text{H}_2\text{O}_2$ - $\text{NH}_3$  solution is also demonstrated in this paper. The resulting products were fully characterized. The

photocatalytic activities of different samples for oxidation of toluene were found to be correlated with the crystal shapes of the rutile TiO<sub>2</sub> nanorods. We demonstrated that the crystal surface structure of TiO<sub>2</sub> nanorods can be controlled by adjusting the etching time of H<sub>2</sub>O<sub>2</sub>-NH<sub>3</sub> or H<sub>2</sub>SO<sub>4</sub> solution. These TiO<sub>2</sub> nanorods are expected to show high levels of photocatalytic activity due to the different crystal faces.

## **2. Experimental**

### **2.1. Chemicals.**

All of the chemical reagents used in this study were commercial products and were used without further treatment. Titanium trichloride (TiCl<sub>3</sub>), sodium chloride (NaCl), hydrogen peroxide (H<sub>2</sub>O<sub>2</sub>), ammonia solution (NH<sub>3</sub>), sulfuric acid (H<sub>2</sub>SO<sub>4</sub>), lead nitrate (Pb(NO<sub>3</sub>)<sub>2</sub>), and nitric acid (HNO<sub>3</sub>) were purchased from Wako (all of reagent grade), and toluene was purchased from Aldrich. TiO<sub>2</sub> (MT-600B, Tayca), a rutile with an average surface area of 25-35 m<sup>2</sup> g<sup>-1</sup>, was used as a reference photocatalyst.

### **2.2. Procedure for chemical etching**

The starting material for rutile TiO<sub>2</sub> nanorods was synthesized by using aqueous

titanium trichloride ( $\text{TiCl}_3$ , 0.15 M) solution containing sodium chloride ( $\text{NaCl}$ , 5 M) with hydrothermal treatment at 200 °C for 6 h [11].

To aqueous hydrogen peroxide ( $\text{H}_2\text{O}_2$ , 30%; 50 mL) in a flask was added aqueous ammonia ( $\text{NH}_3$ , 2.5%; 5.0 mL) under magnetic stirring. A synthesized rutile  $\text{TiO}_2$  (0.5 g) was added to the  $\text{H}_2\text{O}_2$ - $\text{NH}_3$  mixed solution and stirred for 0.5 h to 4 h at room temperature. After such treatment, the  $\text{TiO}_2$  particles were separated by filtration, washed with water several times, and dried at 70 °C in air.

For treatment of  $\text{TiO}_2$  particles with sulfuric acid, concentrated sulfuric acid was used as obtained. For etching with sulfuric acid,  $\text{TiO}_2$  powder (0.5 g) was added to a flask containing sulfuric acid (20 mL) at room temperature. The mixture was stirred for 6 h to 1 week. After the treatment, the  $\text{TiO}_2$  particles were filtered and washed with 1% aqueous ammonia solution and then with deionized water.

### **2.3. Characterization**

The morphology of the samples was observed by field emission scanning electron microscopy (FE-SEM; JEOL, JSM-6701FONO) and transmission electron microscopy (TEM; Hitachi, H-9000NAR). The specific surface area was determined with a surface area analyzer (Quantachrome, Autosorb-1) by using the Brunauer-Emmett-Teller

method [12].

The crystal structures of the powders were confirmed by using an X-ray diffractometer (Rigaku, MiniFlex II) with Cu K $\alpha$  radiation ( $\lambda = 1.5405 \text{ \AA}$ ). Crystal structures of TiO<sub>2</sub> nanorods etched by H<sub>2</sub>O<sub>2</sub> with NH<sub>3</sub> or H<sub>2</sub>SO<sub>4</sub> retained the rutile phase. No peak assigned to anatase or brookite phase after chemical etching was observed by XRD analyses (data not shown).

#### **2.4. Photocatalytic activity measurements**

Photocatalytic activities of rutile TiO<sub>2</sub> nanorods before and after etching treatment were evaluated by measuring the changes in concentrations of toluene in gas phase. At the same time, the amount of evolved CO<sub>2</sub> as a result of photocatalytic mineralization of toluene was also observed by GC as a function of irradiation time.

A Tedlar bag (AS ONE Co. Ltd.) was used as the photoreactor vessel. One hundred mg of TiO<sub>2</sub> powder was spread on the bottom of a glass dish and the dish was placed in a reaction vessel with a volume of 125 cm<sup>3</sup>. Then 100 ppm of toluene was prepared in the vessel by injection of saturated toluene gas. Irradiation was conducted at room temperature after an equilibrium between the gas and the adsorbed toluene had been reached. A 500 W Xe-lamp (USHIO Co. Ltd., SX-UI501XQ) was used as a light source.



The light beam was passed through a UV-35 filter to cut off wavelengths shorter than 350 nm. Fine stainless meshes were used as neutral density filters to adjust the irradiation intensity ( $30 \text{ mW cm}^{-2}$ ). After the irradiation was started, the evolved carbon dioxide concentration was measured using a gas chromatograph (Shimadzu Model GC-8A and GC 14A) equipped with a Flame Ionization Detector (FID) and a methanizer (GL Sciences, MT-221). Toluene was analyzed by a gas chromatograph (Shimadzu GC-1700AF) equipped with an FID and a TC-1 capillary column (length, 30 m; i.d., 0.25 mm; film thickness, 0.25  $\mu\text{m}$ ).

### **3. Results and discussion**

#### ***3.1. Rutile $\text{TiO}_2$ nanorod etching in $\text{H}_2\text{O}_2$ - $\text{NH}_3$ solution***

Rutile  $\text{TiO}_2$  can be dissolved in  $\text{H}_2\text{O}_2$ - $\text{NH}_3$  mixed solution. Ohtani et al. reported that separation of anatase was achieved by selective dissolution of rutile from P25 [10]. They also reported that the rate of rutile dissolution was faster than that of anatase in an  $\text{H}_2\text{O}_2$ - $\text{NH}_3$  mixture. We therefore used a small amount of  $\text{NH}_3$  solution to prevent complete dissolution of rutile  $\text{TiO}_2$  nanorods prepared by the hydrothermal process.

$\text{TiO}_2$  powder (0.5 g) was suspended in a  $\text{H}_2\text{O}_2$ - $\text{NH}_3$  mixed solution (50 mL) and the

mixture was stirred for 0.5 h to 4 h at room temperature, leading to dissolution of the solid to give a light-yellow sol. According to Ohtani et al. [10], the yellow color of the solution during and after treatment suggested the formation of a  $\text{Ti}^{4+}$ - $\text{H}_2\text{O}_2$  complex. Ohtani et al. also suggested that  $\text{NH}_3$  might enhance the selective dissolution of rutile  $\text{TiO}_2$ . TEM and SEM observations revealed that the addition of a small amount of  $\text{NH}_3$  resulted in dissolution of the rutile powder. In the mixture containing 5.0 mL of aqueous 2.5%  $\text{NH}_3$ , the dissolution proceeded rapidly in the initial 0.5 h and then proceeded gradually. We used synthesized rutile  $\text{TiO}_2$  nanorods ( $\text{TiCl}_3$ -0.15 M and  $\text{NaCl}$ -5 M) to observe the crystal faces formed on  $\text{TiO}_2$  particles [11]. Figure 1 shows TEM and SEM images of a rutile  $\text{TiO}_2$  nanorod prepared according to reference [11]. The assignment of crystal faces was reported previously [11]. SEM and TEM images of the rutile  $\text{TiO}_2$  nanorod after treatment with  $\text{H}_2\text{O}_2$ - $\text{NH}_3$  mixed solution for different time periods are shown in Figure 2. The etching rate in  $\text{H}_2\text{O}_2$ - $\text{NH}_3$  solution was very fast. By comparing the structure with that before etching (Fig. 1), we found that the end of the rutile  $\text{TiO}_2$  nanorod is selectively etched with increased reaction time. As a result, the tip of the rutile  $\text{TiO}_2$  nanorod becomes a sepal-like structure after a reaction time of 4 h. However, when the reaction time was increased from 0.5 h to 4 h, the rutile  $\text{TiO}_2$  structure became thinner. As previously reported [11, 13], SAED patterns of the exposed surface of the

end of the rod and side surfaces of the rod were assigned to (111) and to (001) and (110), respectively (data not shown). The areas of exposed (111) and (001) crystal faces gradually decreased with increase in reaction time. At the same time, a cone-shaped rod end was newly exposed and a crystal face assigned to the (110) face gradually decreased as shown in Figure 2.

To determine the site at which oxidation predominantly proceeds, we carried out photodeposition studies of  $\text{PbO}_2$ .  $\text{PbO}_2$  was deposited on the oxidation site of  $\text{TiO}_2$  by oxidation of  $\text{Pb}^{2+}$  ions dissolved in aqueous phase, as was reported previously [11, 14]. Figure 3 shows TEM and SEM images of  $\text{PbO}_2$ -deposited rutile  $\text{TiO}_2$  nanorods that were prepared with 1 h of etching time. The deposited  $\text{PbO}_2$  was analyzed by EDX (figure not shown). In previous papers [11, 14], we presented TEM and SEM images of rutile  $\text{TiO}_2$  particles showing  $\text{PbO}_2$  deposits, which were loaded on the particles by UV irradiation of the Pt-deposited  $\text{TiO}_2$  powder. However, in this study, we only confirmed the oxidation site by using  $\text{PbO}_2$  deposition technique because the number of reduction sites of rutile nanorod treated with  $\text{H}_2\text{O}_2$ - $\text{NH}_3$  solution remarkably decreased. Therefore, assignment of reduction site of rutile nanorod by Pt deposition is rather difficult. Figure 3 shows that the  $\text{PbO}_2$  particles were deposited on the (111) and (001) faces. The results shown in Figure 3 indicate that the oxidation sites on the rutile particles are on the

exposed new cone-shaped rod ends. These results agree with the results of our previous studies [11, 14]. Therefore, the results suggest that effective separation of oxidation sites of rutile TiO<sub>2</sub> nanorods is an important factor for high efficiency of decomposition of toluene.

### **3.2. Rutile TiO<sub>2</sub> etching in H<sub>2</sub>SO<sub>4</sub> solution**

In studies of photoelectrochemistry of a TiO<sub>2</sub> electrode, in order to remove surface damage, researches after treat rutile crystals with concentrated sulfuric acid at about 200-250 °C before measurements [15]. Ohno et al. reported that similar H<sub>2</sub>SO<sub>4</sub> treatment at 200 °C generated new faces of rutile particles [9]. We tried this treatment for TiO<sub>2</sub> powder containing rutile particles. However, the color of rutile TiO<sub>2</sub> particles changed from white to pale gray and the shape of the particles began to deform at high temperatures (100 °C and 200 °C) as shown in Fig. 4. It is plausible that the sizes of TiO<sub>2</sub> particles in our study are smaller than those reported previously [9]. The conditions for etching of TiO<sub>2</sub> nanorods by sulfuric acid are thought to be too severe to expose new crystal faces. Therefore, we tried sulfuric acid treatment for the rutile TiO<sub>2</sub> powder at room temperature. Figure 5 shows TEM and SEM images of rutile particles after sulfuric acid treatment for different time periods. TEM and SEM images before

etching (Fig. 1) revealed that the structures were nanorods with triangular-like tips. The (001) face was exposed as a result of dissolution of the (111) face by H<sub>2</sub>SO<sub>4</sub> etching, its shape is similar to that of rutile TiO<sub>2</sub> synthesized using PVP in the previous study [14]. When the period of etching was increased from 6 h to 72 h, the shape of the end of the rod changed from a triangular-like tip (composed of four triangular-shaped faces with one vertex) to a trapezoid-like tip (composed of four trapezoidal-shaped faces and one square top) (Fig. 5). At the same time, generation of another new face began. After treatment for one week, a different kind of new face had developed on each particle. As seen in Figures 5e and 5e', this new face is assigned to the (021) face, which had been already assigned from a previous paper [9]. As a result, (001) and (021) faces are generated at the tip of TiO<sub>2</sub> and, at the same time, the (111) face disappears from the rutile particle. However, no change in the (110) face of the rutile TiO<sub>2</sub> particle was detected after treatment. Consequently, the surface morphology of the rutile TiO<sub>2</sub> rod was controlled by changing the etching period.

### **3.3. Photocatalytic activity for toluene decomposition**

Figure 6 shows photocatalytic evolution of CO<sub>2</sub> as a result of degradation of toluene on rutile TiO<sub>2</sub> particles after etching at light intensity of 30 mW cm<sup>-2</sup>.

Photocatalytic activity levels of etched  $\text{TiO}_2$  were much higher than those of MT-600B (reference  $\text{TiO}_2$ ) and those before etching of  $\text{TiO}_2$ . Photocatalytic activity levels of  $\text{TiO}_2$  nanorods after etching were higher than those of  $\text{TiO}_2$  nanorods prepared before etching. The photocatalytic activity of the  $\text{TiO}_2$  particles showed dependence on the time of etching, though  $S_{\text{BET}}$  showed no dependence on the etching period (see Table 1). These results suggest that the particle size or the surface area does not play an important role in this reaction. The newly exposed crystal surface or the ratio of oxidation and reduction sites is an important factor for improvement of photocatalytic activity of toluene degradation.

Figure 6a shows the time course of  $\text{CO}_2$  evolution in degradation of toluene over  $\text{TiO}_2$  particles before and after treatment with  $\text{H}_2\text{O}_2\text{-NH}_3$  solution. With  $\text{H}_2\text{O}_2\text{-NH}_3$  treatment, the activities of toluene were higher than those before etching, suggesting that etching is effective for improving toluene oxidation. The effect of  $\text{H}_2\text{O}_2\text{-NH}_3$  treatment was significant for a reaction time of 1 h.  $\text{TiO}_2$  etched with 1 h of reaction time showed the highest photocatalytic activity among the treatments of  $\text{TiO}_2$  samples even though all had similar surface areas. Our results suggest that the balance between oxidation and reduction sites is important for high photocatalytic activity in the  $\text{H}_2\text{O}_2\text{-NH}_3$  etching method. The rate-determining step of the reaction is thought to be, not

reduction of oxygen by photoexcited electrons, but oxidation of toluene by holes generated photocatalytically because toluene is difficult to oxidize. Therefore, it is thought that photocatalytic activity of a rutile TiO<sub>2</sub> nanorod increases with increase in the oxidation sites on the rutile TiO<sub>2</sub> nanorod. The results suggest that there is a synergetic effect between oxidation and reduction sites in etched TiO<sub>2</sub> particles in H<sub>2</sub>O<sub>2</sub>-NH<sub>3</sub> solutions.

Figure 6b shows the time course of CO<sub>2</sub> evolution in degradation of toluene over TiO<sub>2</sub> particles before and after treatment with an H<sub>2</sub>SO<sub>4</sub> solution. As-synthesized rutile TiO<sub>2</sub> nanorods with PVP exposed by (001) faces have been shown to have high photocatalytic efficiency [14]. In this experiment, we expected high photocatalytic activities to be exhibited because of similar shaped TiO<sub>2</sub> prepared by hydrothermal method with PVP [14]. Commercially available MT-600B TiO<sub>2</sub> was also used as a reference for comparison. It was found that etched TiO<sub>2</sub> particles exhibited a higher degradation rate of toluene than that before etching and that the degradation efficiency was higher than that of reference TiO<sub>2</sub>. Furthermore, we expected that the etched TiO<sub>2</sub> particles with a higher percentage of (001) faces would have photocatalytic performance, demonstrating high catalytic activity of the (001) face with strong oxidation sites. However, TiO<sub>2</sub> etched with 15 h of reaction time in H<sub>2</sub>SO<sub>4</sub> solution

showed the highest photocatalytic activity among the etched TiO<sub>2</sub> particles, despite a small exposed (001) face. Under this etching condition, the new exposed crystal face, (001), was thought to play an important role in improvement of photocatalytic activity of rutile TiO<sub>2</sub> nanorods. We previously reported that the exposed crystal face, (001), showed stronger oxidation power than that of the (111) crystal face [14]. TiO<sub>2</sub> etched for longer than 15 h showed lower photocatalytic activity than that of TiO<sub>2</sub> etched for 15 h despite having a larger (001) exposed crystal face. A possible reason for this is that the (021) newly exposed surface on etched TiO<sub>2</sub>, which is shown in SEM images in Figure 5, might prevent oxidation reaction of reactants, resulting in a decrease in the efficiency of photocatalytic reaction. However, our results suggest that the photocatalytic activity of the samples for toluene degradation was affected by the newly exposed crystal surface of rutile TiO<sub>2</sub>.

#### **4. Conclusion**

We have demonstrated that the surface structure of TiO<sub>2</sub> particles can be controlled by means of chemical etching. The etched TiO<sub>2</sub> particles showed high photocatalytic activities due to newly exposed crystal faces. Addition of reagents of chemical etching enabled control of the exposed crystal faces of rutile TiO<sub>2</sub> nanorods in crystallization.



The morphology of rutile crystals can be controlled by changing the reagent of chemical etching and the etching period. We showed that etched rutile TiO<sub>2</sub> possessed higher levels of CO<sub>2</sub> evolution activity than those of MT-600B and TiO<sub>2</sub> without treatment of chemical etching under UV light irradiation. It was found that the photocatalytic activity depends not on surface area but on surface structure of the TiO<sub>2</sub> nanorods, suggesting that electron-hole pair recombination plays an important role during the photodegradation of toluene, at least under the present experimental conditions.

## **Acknowledgements**

This work was partly supported by a grant of Knowledge of Cluster Initiative implemented by the Ministry of Education, Culture, Sports, Science and Technology (MEXT) and the New Energy and Industrial Technology Development Organization (NEDO).

## References

- [1] C.B. Mendive, T. Bredow, A. Feldhoff, M. Blesa, D. Bahnemann, *Phys. Chem. Chem. Phys.* 10 (2008) 1960-1974.
- [2] E. Hosono, S. Fujihara, K. Kakiuchi, H. Imai, *J. Am. Chem. Soc.* 126 (2004) 7790-7791.
- [3] X. Chen, S.S. Mao, *Chem. Rev.* 107 (2007) 2891-2959.
- [4] N.R. Neale, A.J. Frank, *J. Mater. Chem.* 17 (2007) 3216-3221.
- [5] X. Huang, C. Pan, *J. Cryst. Growth* 306 (2007) 117-122.
- [6] R.L. Whetten, *Mater. Sci. Eng. B* 19 (1993) 8-13.
- [7] L.A. Harris, R.H. Wilson, *J. Electrochem. Soc.* 123 (1976) 1010-1015.
- [8] Y. Nakato, H. Akanuma, J.-i. Shimizu, Y. Magari, *J. Electroanal. Chem.* 396 (1995) 35-39.
- [9] T. Taguchi, Y. Saito, K. Sarukawa, T. Ohno, M. Matsumura, *New J. Chem.* 27 (2003) 1304-1306.
- [10] B. Ohtani, Y. Azuma, D. Li, T. Ihara, R. Abe, *Trans. Materials Res. Soc. Jpn.* 32 (2007) 401-404.
- [11] E. Bae, N. Murakami, T. Ohno, *J. Mol. Catal. A: Chem.* 300 (2009) 72-79.
- [12] C. Ribeiro, C. Vila, D.B. Stroppa, V.R. Mastelaro, J. Bettini, E. Longo, E.R.

Leite, J. Phys. Chem. C 111 (2007) 5871-5875.

[13] E. Bae, N. Murakami, T. Ohno, J. Mol. Catal. A 300 (2009) 72-79.

[14] E. Bae, T. Ohno, Appl. Catal. B: Environ. 91 (2009) 634-639.

[15] M.P. Dare-Edwards, A. Hamnett, J. Electroanal. Chem. 105 (1979) 283-290.

**Table 1.** Specific surface areas of rutile TiO<sub>2</sub> nanorod samples.

Sample	Conditions	BET surface area (m <sup>2</sup> /g)
MT-600B		25-35
Before etching		18.6
H <sub>2</sub> O <sub>2</sub> -NH <sub>3</sub> -0.5h	0.5h stirring	16.1
H <sub>2</sub> O <sub>2</sub> -NH <sub>3</sub> -1h	1h stirring	15.3
H <sub>2</sub> O <sub>2</sub> -NH <sub>3</sub> -2h	2h stirring	15.9
H <sub>2</sub> O <sub>2</sub> -NH <sub>3</sub> -4h	4h stirring	15.3
H <sub>2</sub> SO <sub>4</sub> -6h	6h stirring	17.4
H <sub>2</sub> SO <sub>4</sub> -15h	15h stirring	15.7
H <sub>2</sub> SO <sub>4</sub> -24h	24h stirring	18.5
H <sub>2</sub> SO <sub>4</sub> -72h	72h stirring	16.6
H <sub>2</sub> SO <sub>4</sub> -1 week	168h stirring	17.0

## Figure Captions

**Figure 1.** (a) TEM image and (b) SEM image of rutile particles present in the TiO<sub>2</sub> powder used in this study.

**Figure 2.** TEM images and SEM images of rutile particles after treatment with aqueous H<sub>2</sub>O<sub>2</sub>-NH<sub>3</sub> solution. The etching periods were about (a) 0.5 h, (b) 1 h, (c) 2 h and (d) 4 h.

**Figure 3.** (a) TEM image and (b) SEM image of a rutile TiO<sub>2</sub> nanorod (H<sub>2</sub>O<sub>2</sub>-NH<sub>3</sub>-1h) on which PbO<sub>2</sub> particles were photodeposited.

**Figure 4.** TEM image of rutile particle after treatment with sulfuric acid at 200 °C.

**Figure 5.** TEM images and SEM images of rutile particles after treatment with sulfuric acid. The etching periods were about (a) 6 h, (b) 15 h, (c) 24 h, (d) 72 h and (e) 1 week.

**Figure 6.** Time profiles of CO<sub>2</sub> evolution of toluene decomposition over TiO<sub>2</sub> particles prepared by treatment with (a) H<sub>2</sub>O<sub>2</sub>-NH<sub>3</sub> and (b) sulfuric acid at light intensity of 30 mW cm<sup>-2</sup>. The experimental conditions were: [toluene]<sub>i</sub> = 100 ppm, [TiO<sub>2</sub>] = 10.4 mg/cm<sup>2</sup>, UV light ( $\lambda > 350$  nm) irradiated.

Figure(s)  
[Click here to download high resolution image](#)

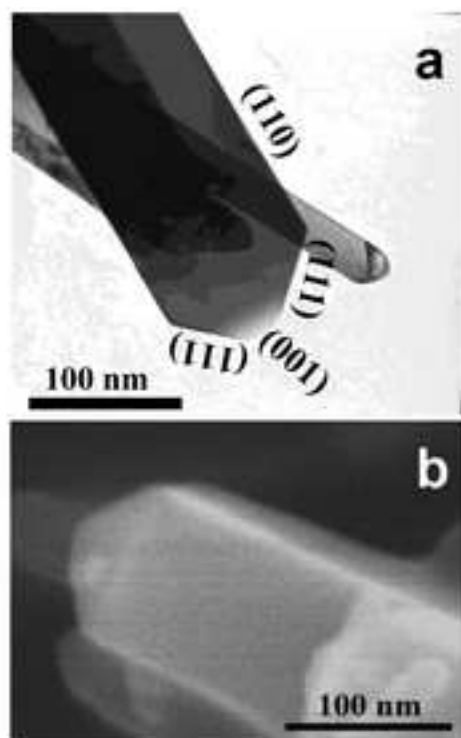


Figure 1.

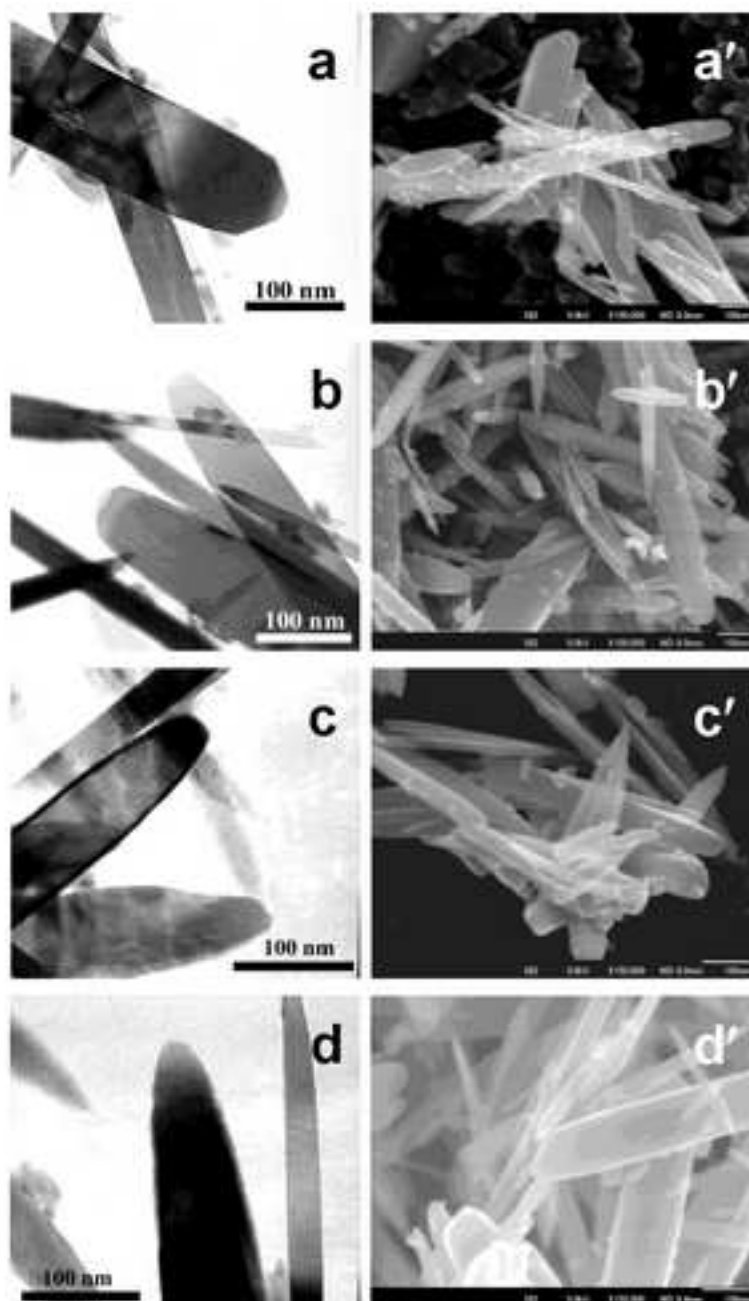


Figure 2.

Figure(s)  
[Click here to download high resolution image](#)

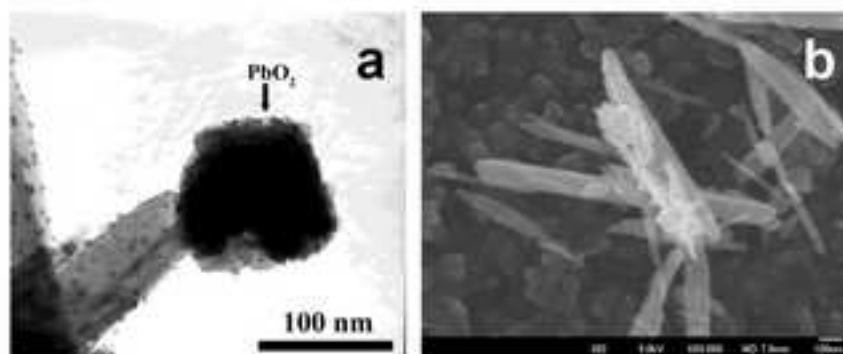


Figure 3.



Figure(s)

[Click here to download high resolution image](#)

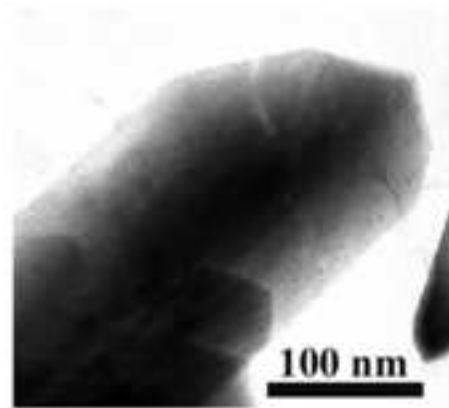


Figure 4.

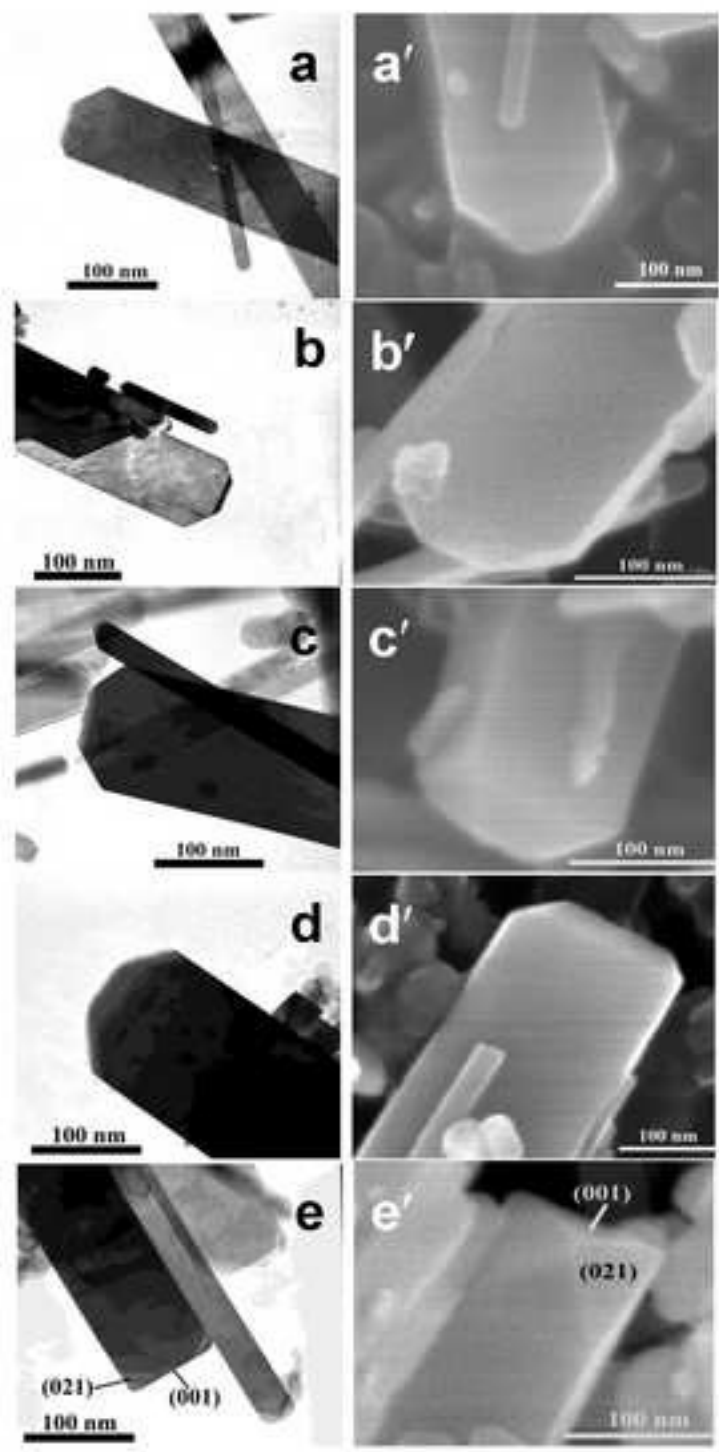


Figure 5.

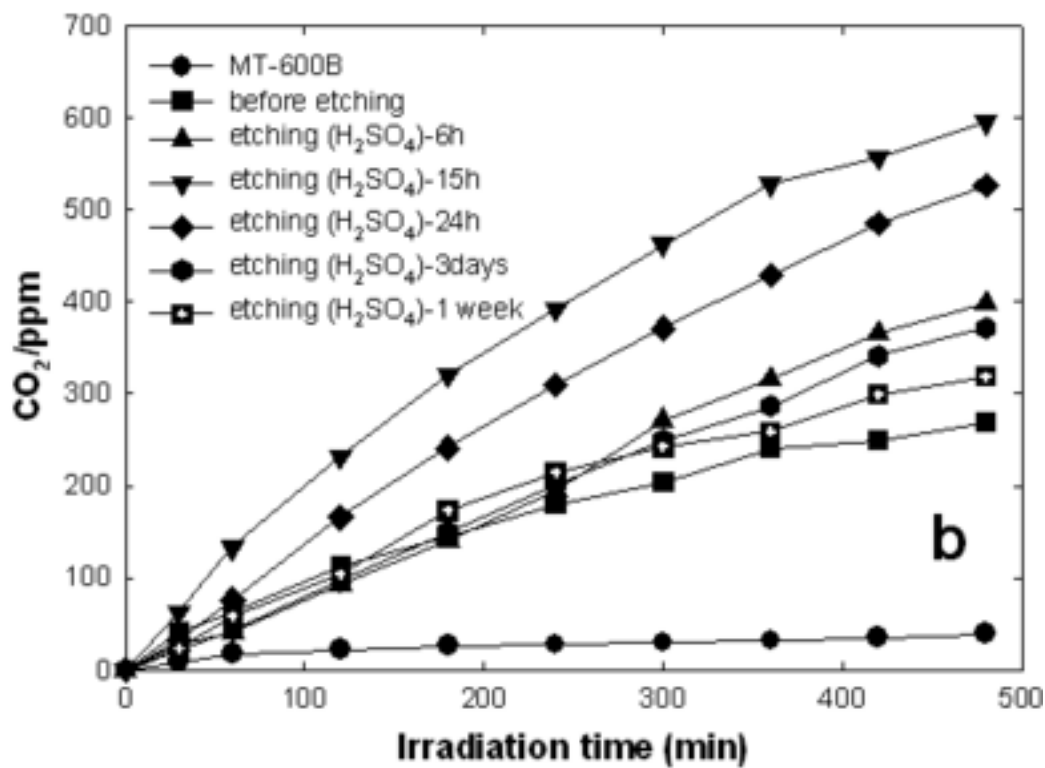
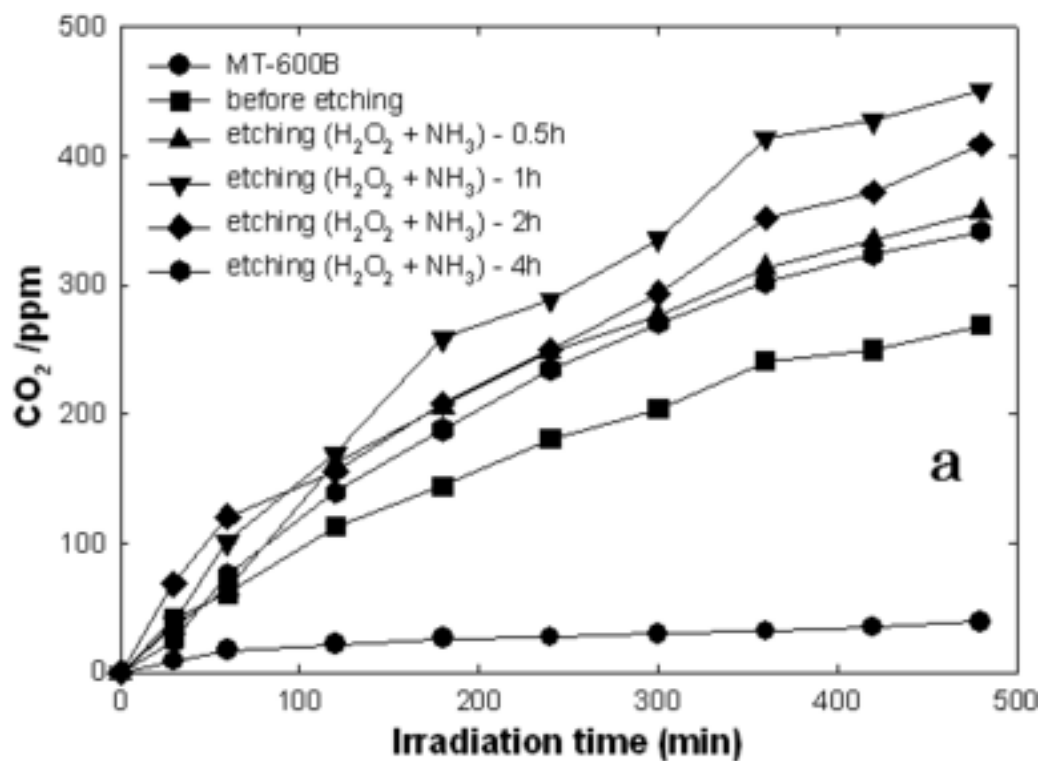


Figure 6.